Supporting Information for

Original Article

Remodeling "cold" tumor immune microenvironment *via* epigenetic-based therapy using targeted liposomes with *in situ* formed albumin corona

Yang He[a,b,c,d,†], Yuefei Fang[a,e,†], Meng Zhang[a,f], Yuge Zhao[a], Bin Tu[a,b], Mingjie Shi[a], Bahtiyor Muhitdinov[a,g], Akmal Asrorov[a,g], Qin Xu[e], Yongzhuo Huang[a,b,c,h,*]

[a]*State Key Laboratory of Drug Research, Shanghai Institute of Materia Medica, Chinese Academy of Sciences, Shanghai 201203, China*

[b]*University of Chinese Academy of Sciences, Beijing 100049, China*

[c]*Zhongshan Institute for Drug Discovery, Shanghai Institute of Materia Medica, Chinese Academy of Sciences, Zhongshan 528437, China*

[d]*Department of Pharmacy, the First Affiliated Hospital of Zhengzhou University, Zhengzhou 450052, China*

[e]*Artemisinin Research Center, Guangzhou University of Chinese Medicine, Guangzhou 510450, China*

[f]*Women's Hospital, School of Medicine, Zhejiang University, Hangzhou 310006, China*

[g]*Institute of Bioorganic Chemistry, Uzbekistan Academy of Sciences, Tashkent 100125, Uzbekistan*

[h]*National Medical Products Administration, Key Laboratory for Quality Research and Evaluation of Pharmaceutical Excipients, Shanghai 201203, China*

Received 27 July 2021; received in revised form 21 September 2021; accepted 22 September 2021

*Corresponding author. Tel./fax: +86 2120231981.

E-mail address: yzhuang@simm.ac.cn (Yongzhuo Huang).

[†]These authors made equal contributions to this work.

Table S1 The HPLC condition of Pano: gradient elution method.

Time (min)	Flow rate (mL/min)	Acetonitrile	0.1% Phosphoric acid	Wavelength (nm)
0	1	5%	95%	280
2		5%	95%	
12		65%	35%	
14		5%	95%	
15		5%	95%	

Table S2 The HPLC condition of JQ1: isocratic elution method.

Flow rate (mL/min)	H_2O	Acetonitrile	Wavelength (nm)
1	40%	60%	254

Table S3 The combination index of various ratios of Pano and JQ1 in CT26 tumor cells.

Pano/JQ1 (molar ratio)	Combination index
4:1	0.64
2:1	0.40
1:1	0.38
1:2	0.25
1:4	0.31

Figure S1 Characterization of the materials. A) Schematic diagram of the synthesis of DSPE-PEG-LF. B) MALDI-TOF of lactoferrin (left), DSPE-PEG-NHS (middle), and DSPE-PEG-LF (right). C) Characteristic ^{1}H-NMR spectra of lactoferrin (top), DSPE-PEG-NHS (middle), and DSPE-PEG-LF (bottom). D) Characteristic ^{13}C-NMR spectra of lactoferrin (top), DSPE-PEG-NHS (middle), and DSPE-PEG-LF (bottom).

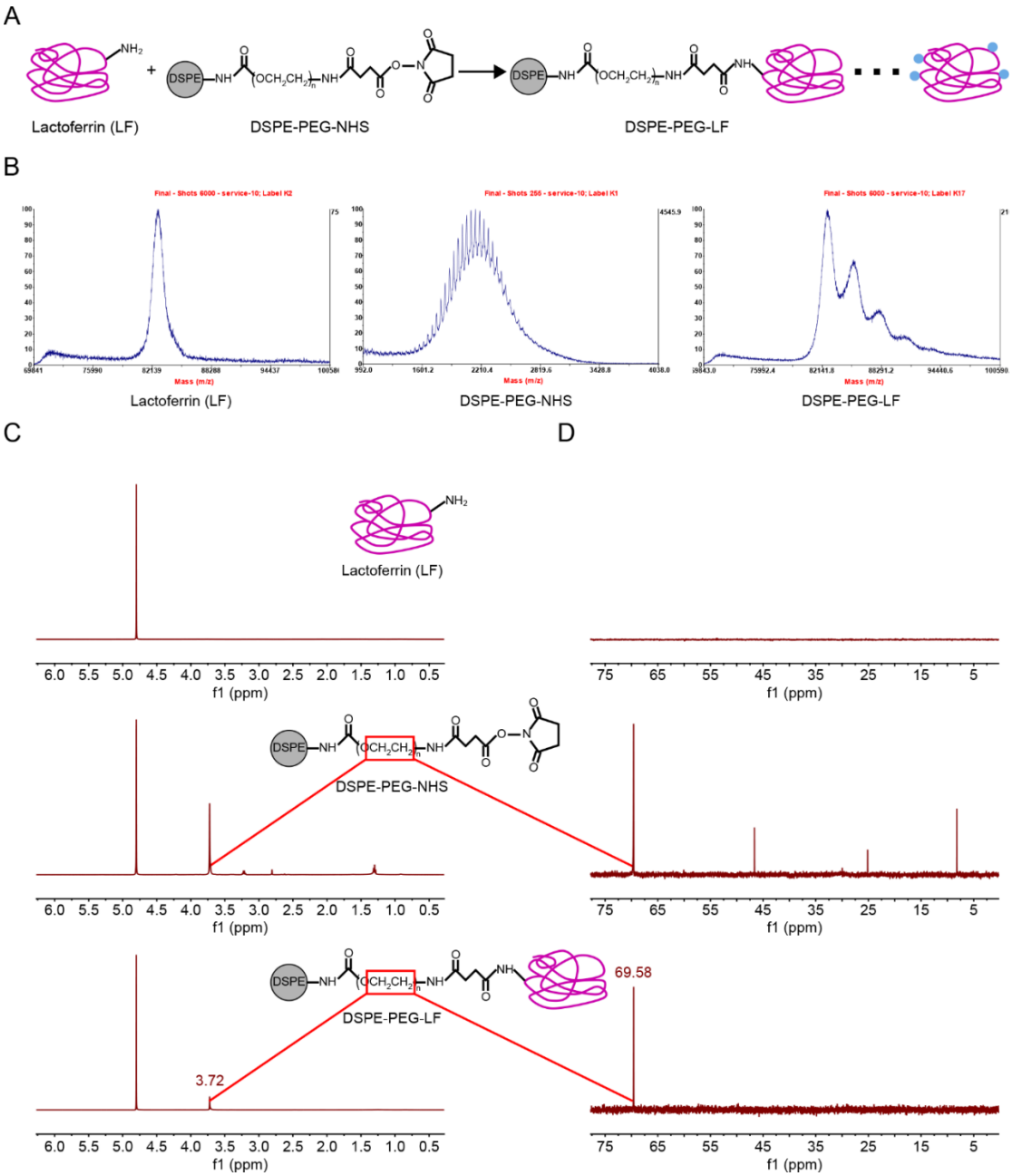

Figure S2 Glycolysis regulation in macrophages after treatment with Pano and JQ1. A) The reduced lactic acid production in M2*Φ* after treatment. B) Expression of PKM2 in M2*Φ* after treatment. Data are presented as mean±SD (*n*=3). $^{**}P<0.01$, $^{****}P<0.0001$.

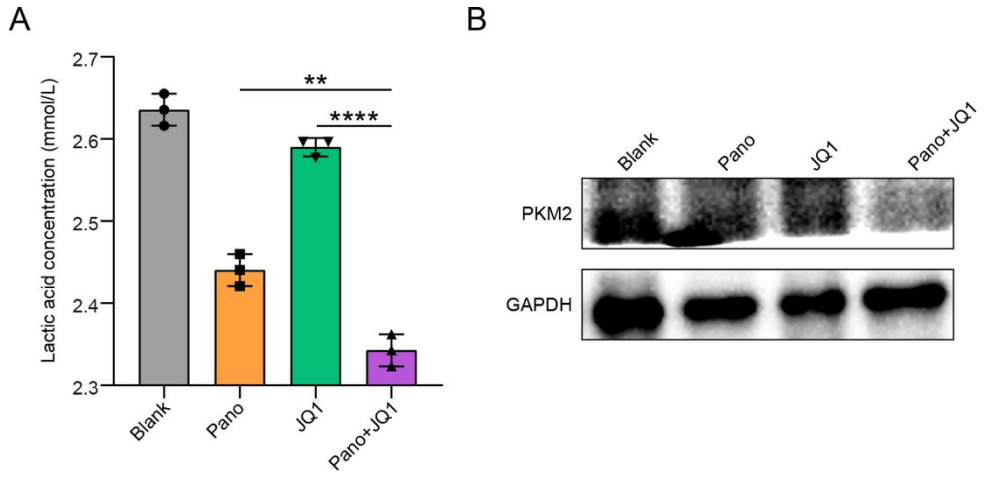

Figure S3 Cellular uptake and *in vitro* cytotoxicity of the liposomes in BMDMs. A) Cellular uptake of Lipo and LF-Lipo in M2*Φ* cells. B) Statistical analysis of cellular uptake efficiency in M2*Φ* cells. C) Cytotoxicity test in BMDMs after treatment. Data are presented as mean ±SD (*n*=3). $^{****}P<0.0001$.

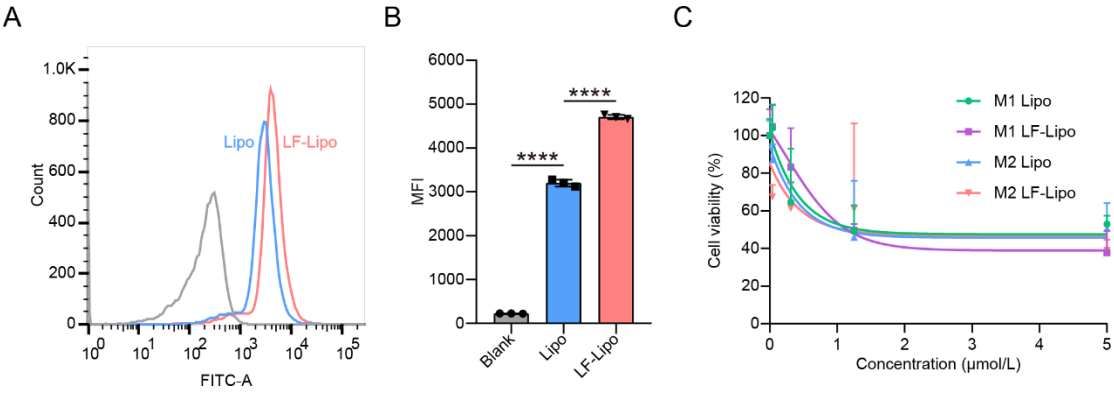

Figure S4 Preliminary safety evaluation in CT26 subcutaneous tumor-bearing mouse model. A) The body weight changes during the treatment. B) The organ coefficients. C) Histological examination of the major organs (scale bar=100 μm). No obvious lesion was found in all groups. Data are presented as mean ±SD (*n*=6).

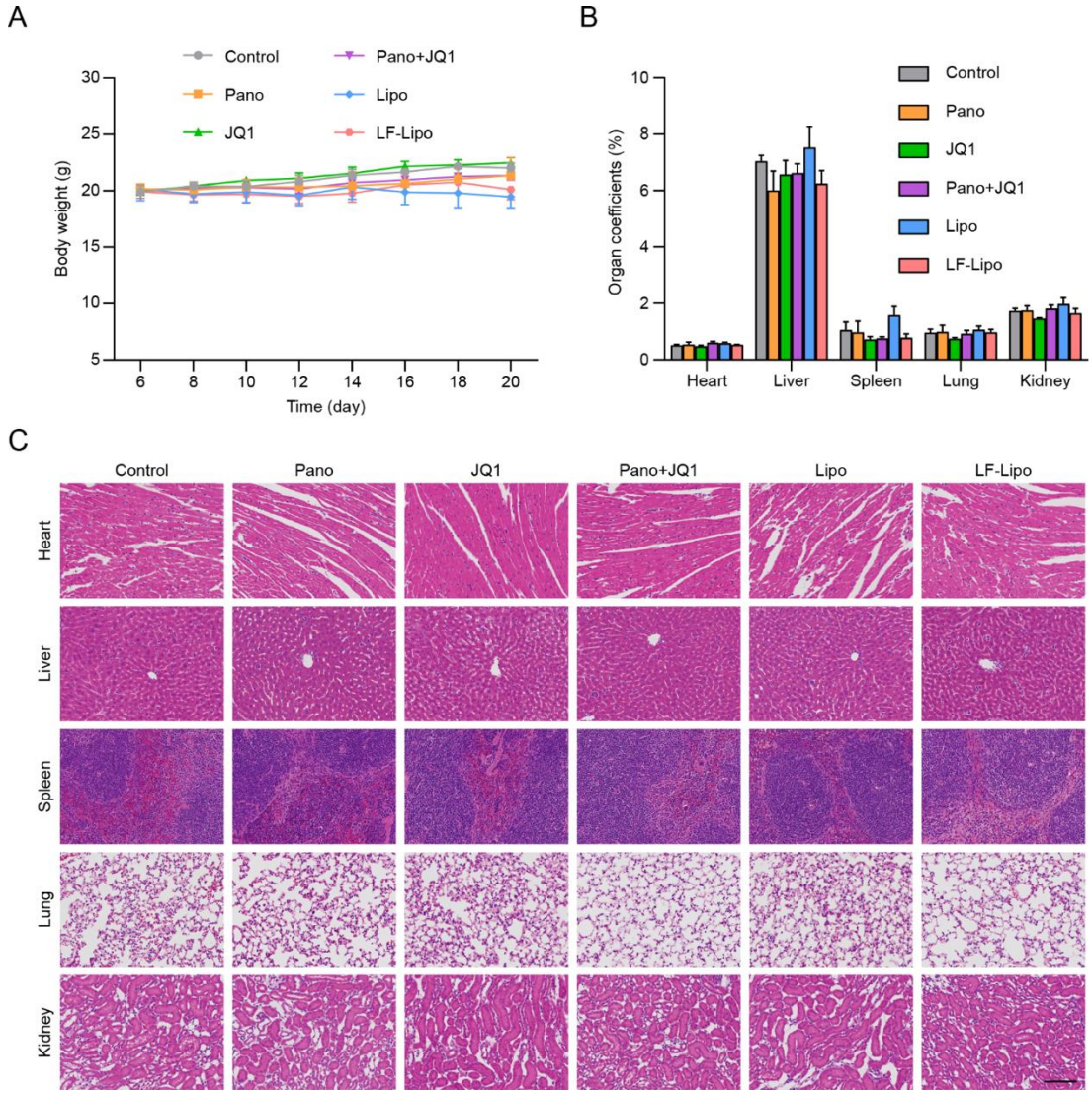

Figure S5 Immune cell assay in the CT26 subcutaneous tumor. The percentage of $CD45^+$ $Gr\text{-}1^+$ (A), $F4/80^+$ $CD206^+$ (B), $CD49b^+$ $NK1.1^+$ (C), $CD8^+$ granzyme B^+ (D) cells in the tumor tissues.

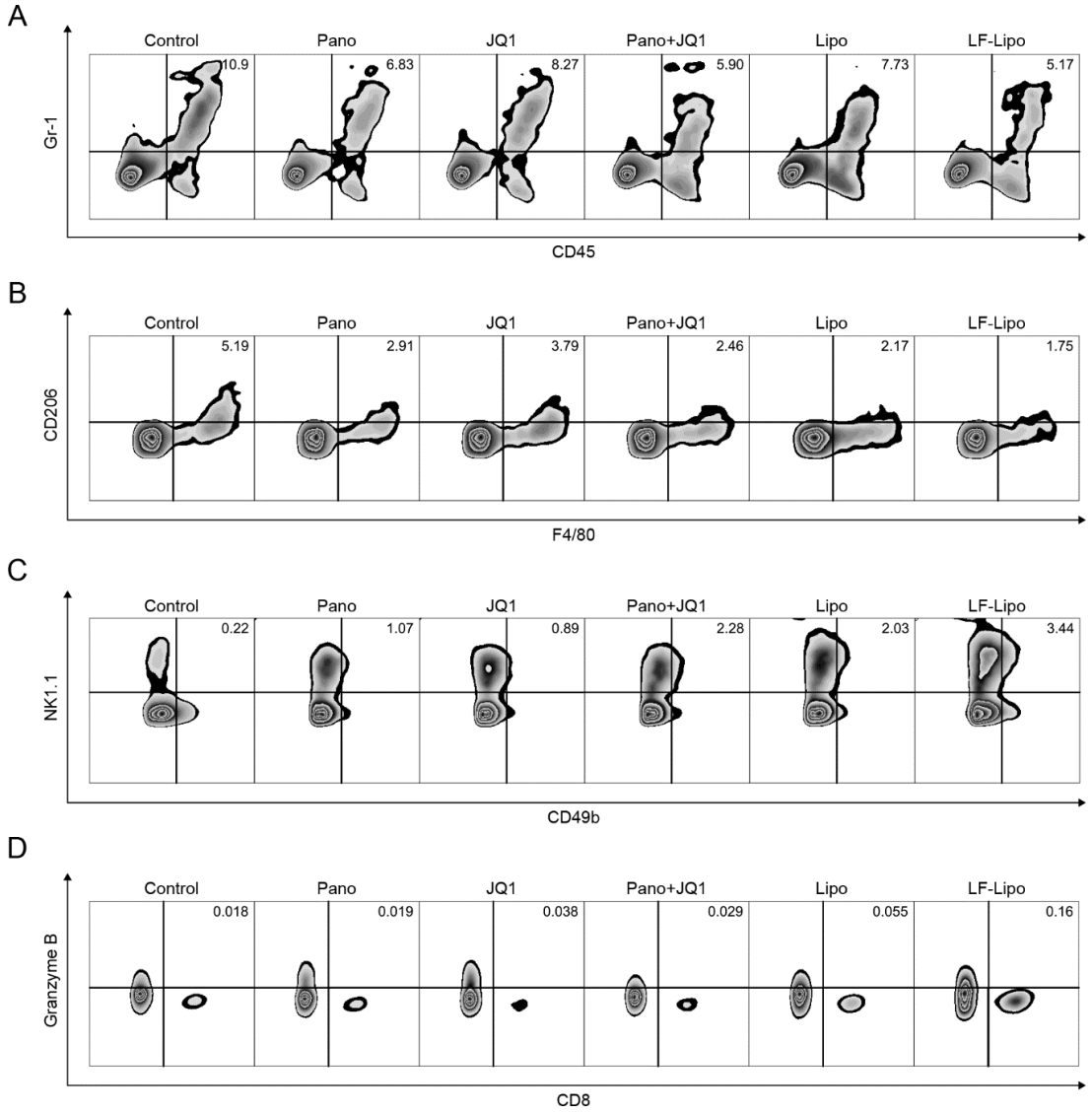

Figure S6 *In vivo* imaging and biodistribution of the liposomes in CT26 peritoneal tumor model. A) Schematic diagram of the detection of the CT26 peritoneal tumor. B) Bioluminescence imaging of CT26 peritoneal tumor. C) *In vivo* imaging from 0.5 h to 24 h. D) *In vivo* real-time radiant efficiency at the tumor sites. E) *Ex vivo* imaging of major organs and CT26 peritoneal tumors. F) *Ex vivo* radiant efficiency of the CT26 peritoneal tumors. Data are presented as mean ±SD (n=3). $^{*}P$<0.05.

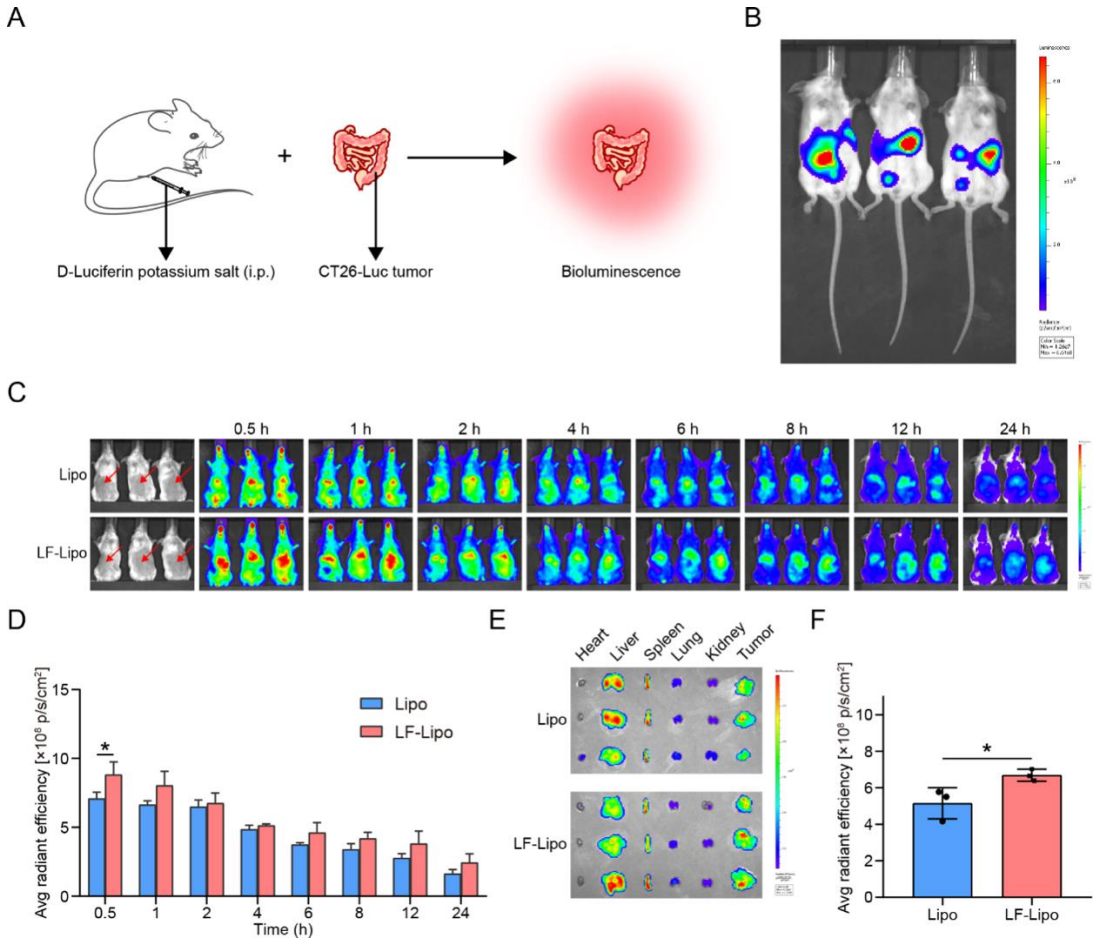

Figure S7 Immunohistochemical staining (brown color) of BRD4, HDAC2, Gr-1, and CD206 in CT26 peritoneal tumors after treatment (scale bar=100 μm).

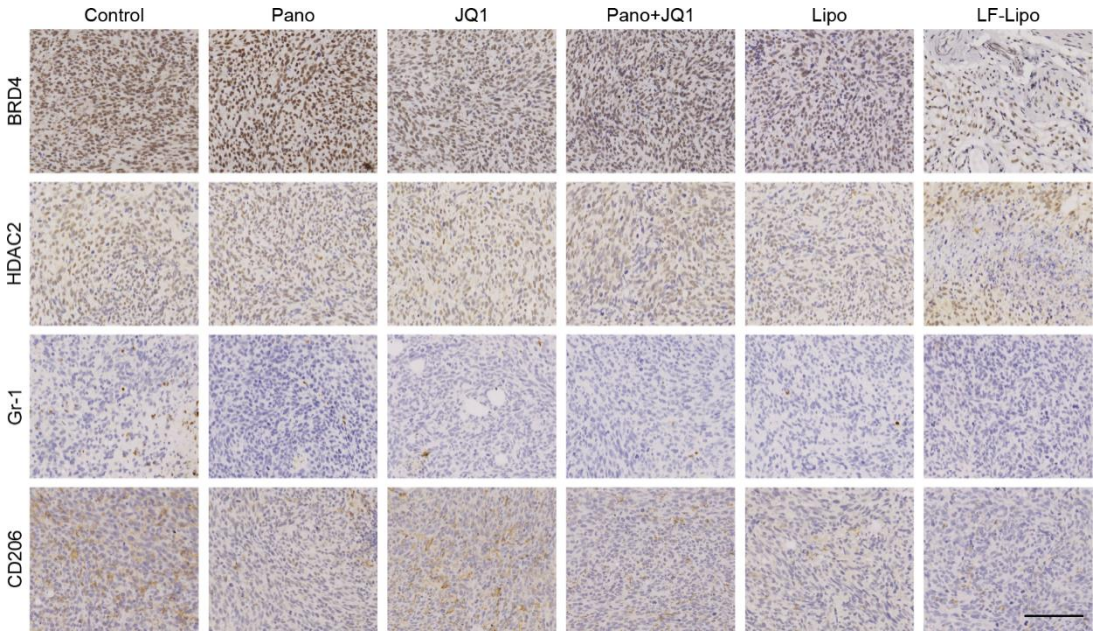

Figure S8 Immune cell assay in the CT26 peritoneal tumor model. The percentage of F4/80$^+$ TGF-β^+ (A), CD8$^+$ granzyme B$^+$ (B), and CD8$^+$ IFN-γ^+ (C) cells in the tumor tissues.